NANO LETTERS

2006
Vol. 6, No. 3
548−551

Anisotropic Etching of SiC Whiskers

Goknur Z. Cambaz,† Gleb N. Yushin,† Yury Gogotsi,*,† and Vadim G. Lutsenko‡

Department of Materials Science and Engineering, Drexel University, 3141 Chestnut Street Lebow Building, Room 344, Philadelphia, Pennsylvania 19104, and V.I. Vernadski Institute of General and Inorganic Chemistrym Ukrainian National Academy of Sciences, 32/34 Prospekt Palladina, 03680 Kiev 142, Ukraine

Received September 16, 2005; Revised Manuscript Received September 28, 2005

ABSTRACT

We have demonstrated a method of producing nanoplatelets or complex well-ordered nanostructures from silicon carbide (SiC) whiskers. Preferential etching of SiC whiskers in a mixture of hydrofluoric and nitric acids (3:1 ratio) at 100 °C results in the selective removal of cubic SiC and the formation of complex structures resembling a pagoda architecture. Possible mechanisms governing selective etching are discussed. Reproducible results on SiC whiskers manufactured in different laboratories suggest that the self-patterning phenomena are common in SiC whiskers, and the same electroless etching procedure can be used to synthesize various complex nanostructures from more conventional nano- and microscale objects for use as building blocks in the fabrication of sensors, cellular probes, and electronic, optoelectronic, electromechanical, and other devices.

The development of low-cost lithographical patterning processes on the nanoscale level remains a great technological challenge, particularly when complex three-dimensional (3D) nanostructures are to be obtained. Self-assembly or self-organization mechanisms have been applied successfully to the growth of 0D and 1D nanostructures using spontaneous surface patterns, such as surface reconstruction,[1] surface steps,[2] or ordered dislocations at the surface.[3] The growth of more complex 3D nanostructures with ordered features remains a challenge, and the development of new techniques that can manipulate matter on a nanoscale level may potentially be used for the fabrication of nanosized device components. Many applications require making not only small regular structures with shallow features but also nano-objects with larger voids that can capture molecules or nanoparticles; however, research in this area has been very limited.

An on-wire lithography process was proposed recently[4] for making segmented nanowires with nanoscopic gaps. However, it is limited to easily etchable bimetallic structures. Complex shapes, such as spikes with protruding barbs, have been fabricated of Si at the microscale level.[5] However, this method is applicable only to silicon, and no nanoscale structures could be produced. SiC has attracted significant attention as a potential material for high frequency, high power, and high-temperature applications because of its unique electrical and thermal properties, such as a high electric field at breakdown (2×10^6 V cm^{-1}), a high electron velocity (2×10^7 cm s^{-1}), a large band gap (2.3 eV for cubic 3C SiC and 3.2 eV for the hexagonal 4H polytype), and a high thermal conductivity (400 W K^{-1} m^{-1}).[6] Despite its excellent electronic properties, the fabrication of SiC electronic devices with novel designs has been hindered by the chemical inertness of this material. Several dry-etching methods have been proposed and are used commonly for the fabrication of SiC devices.[7,8] However, because of the strong physical component in dry etching, it has a low-etch selectivity between materials and can cause surface damage.[9,10] Wet chemical etching is a desirable substitute for the dry-etching method because it produces negligible damage, can be highly selective, is relatively inexpensive, and can be done with simple equipment. In general, the wet etching of semiconductors involves oxidation of the surface and subsequent dissolution of the oxidized species. Oxidation requires holes to be supplied to the surface either via electrochemical circuit or chemically (by a strong oxidant).[11] As such, wet electroless chemical etching is thermodynamically possible only if the potential of the semiconductor is lower than the redox potential of an oxidizing agent (in other words, if the semiconductor has a smaller affinity for electrons and is prone to giving away electrons to the oxidant). Similarly, the etching rate depends on the position of the semiconductor energy band relative to the energy levels of the redox couple in the solution.[9]

In this work, we demonstrate a method for the low-cost large-scale production of intricate 3D objects and hexagonal platelets by wet chemical etching of self-patterned SiC whiskers.

SiC whiskers grown by two different methods were used in our experiments including industrially produced whiskers[12]

* Corresponding author. E-mail: gogotsi@drexel.edu. Fax: +1 (215) 895-1934. Phone: +1 (215) 895-6446.
† Drexel University.
‡ Ukrainian National Academy of Sciences.

10.1021/nl051858v CCC: $33.50 © 2006 American Chemical Society
Published on Web 10/11/2005

and experimental whiskers produced by carbothermal synthesis on carbon felt.[13] Whiskers were etched electrolessly in the 3:1 mixture of 47−52% HF (Fisher Scientific) and 70% HNO_3 solutions (Acros Organics) at 100 °C for 3 h. After etching, whiskers were subsequently washed with DI water and collected on a polypropylene membrane with a pore size of 0.2 μm. Because the results obtained in the study are very similar for both types of SiC whiskers, the analyses of only one kind of whiskers (Figures1−3) will be demonstrated in this paper.

The morphology of the samples was studied by scanning electron microscopy (SEM), transmission electron microscopy (TEM), and Raman spectroscopy. To separate the agglomerated whiskers, we ultrasonically dispersed them in ethanol for 1 min. Subsequently, a droplet was deposited on a lacey-carbon coated copper grid (200 mesh) for TEM analyses, on Si substrate for SEM, and on an Au-coated substrate for Raman spectroscopy studies.

SEM was performed using a Philips XL-30 environmental field-emission SEM. A 200-kV field-emission TEM (JEOL 2010F) with an imaging filter (Gatan GIF) was used for TEM analyses. Micro-Raman analysis was done using a Ramascope 1000 Raman micro spectrometer (Renishaw, U.K.). An Ar ion laser (λ = 514.5 nm) was employed as an excitation source for Raman studies.

Morphology. Figure 1a−d shows the SEM and TEM micrographs of as-grown SiC whiskers with a hexagonal cross-section, diameter of 50−1000 nm, and an average aspect ratio of 20−40. The dark lines perpendicular to the axis of the nanowhisker (Figure 1d) and the streaks in the selected area diffraction (SAD) pattern of the section shown in Figure 1d suggest the presence of stacking faults along the growth direction. The presence of stacking faults in the grown SiC whiskers is a common phenomenon. The extensive studies of various cubic SiC whiskers[14−16] revealed that the primary defects in these whiskers are stacking faults distributed periodically (or nearly periodically) on the (111) planes perpendicular to the whisker growth axis.

Typical SEM and TEM images of the whiskers after etching are shown in Figure 1e and g, respectively. Clearly, the etching process was very selective to some parts of the whiskers, resulting in the formation of very unusual ordered nanostructures (Figure 1f and h), consisting of ∼10-nm-thick platelets that are strung through an SiC rod. The formed nano-objects mimic some advanced architecture such as Japanese pagodas.

Figure 2a and b shows the SEM and TEM images of hexagonal platelets separated from the whiskers during etching. The contrast variations within the platelets observed by both methods may indicate some thickness variations caused by the etchant. HRTEM analysis (Figure 2c) confirmed that the produced platelets oriented along the basal planes are SiC crystals. The EDS analysis (not shown) of whiskers also showed that they are composed of Si, C, and O and there is no significant difference in the chemical composition of as-grown and etched whiskers.

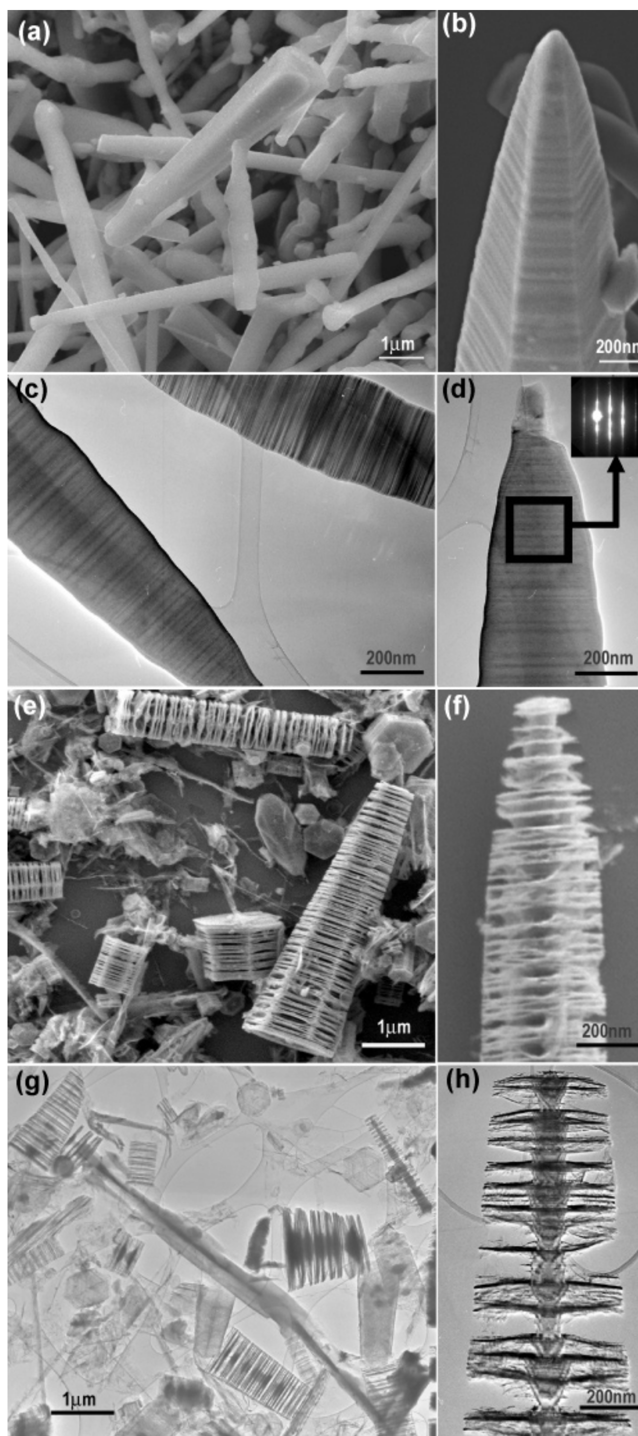

Figure 1. SEM (a and b) and TEM (c and d) micrographs of as-received 3C-SiC whiskers. the inset in d shows an SAD pattern of the selected area. SEM and TEM micrographs of etched SiC whiskers are shown in e and f and g and h, respectively.

Raman Analysis. Figure 3 shows the representative Raman spectra of single SiC whiskers before and after etching. The Raman spectrum of the original whiskers (Figure 3a) showed a single strong peak centered at around 794 cm^{-1}. The position of this peak and the absence of additional peaks of sufficient intensity at lower wavenumbers indicate the cubic (β or 3C) structure of SiC whiskers (Table 1). However, the small downshift of the peak from ∼796 cm^{-1} and asymmetric broadening suggests the presence of stacking faults[17] (which can also be viewed as inclusions of other polytypes), confirming the results of SAD and TEM.

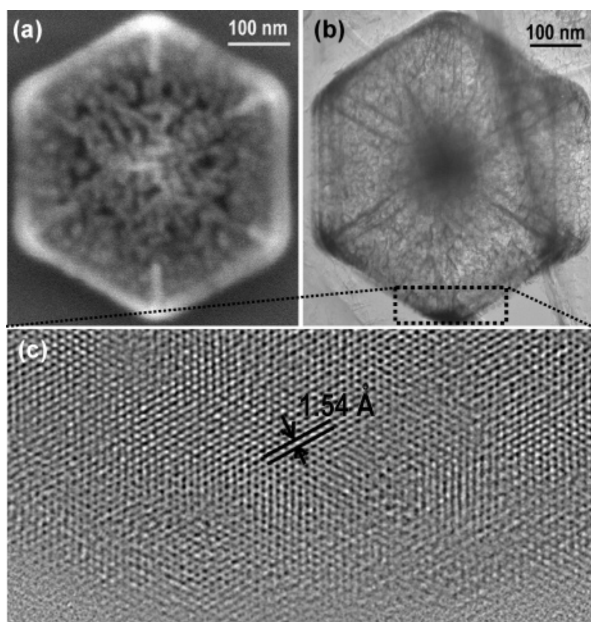

Figure 2. SEM (a) and TEM (b) images of a free-standing SiC platelet showing hexagonal cross section of the etched whiskers. (c) HRTEM image of the framed corner of the hexagonal platelet shown in b.

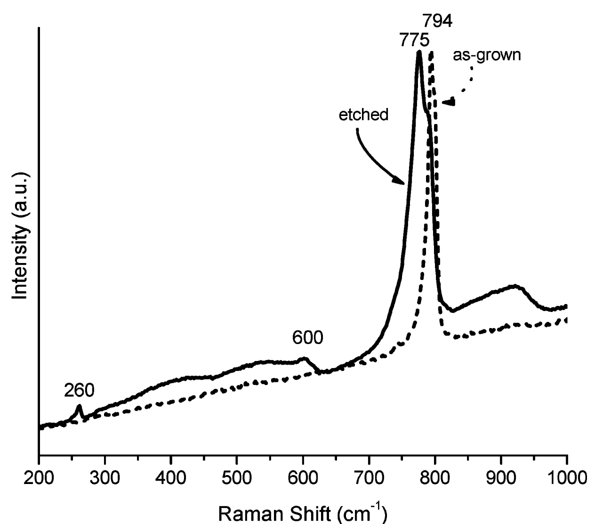

Figure 3. Raman spectra of as-grown (dotted) and etched (solid black line) SiC whiskers.

Upon etching, although no peaks disappeared completely, the whiskers showed a markedly different intensity of Raman peaks. The peak at 794 cm^{-1} became more broadened and downshifted to lower frequency, where α-SiC polytypes' peaks appear (Table 1). Additional characteristic peaks of the alpha phase emerged at low frequencies (∼260 and 600 cm^{-1}). Comparison of the observed spectra to the typical Raman spectra of the most common SiC polytypes (3C, 2H, 4H, 6H, and 15R) reported in the literature[15] suggests that the etched whiskers consist mainly of 4H-SiC. Clearly, the etching dissolved most of the β-SiC present in the as-grown whiskers as shown schematically in Figure 4, leaving stacking fault areas, which can be considered as α-SiC interlayers, behind.

Table 1. Position of Raman Bands for Common SiC Polytypes within a 600−1100 cm^{-1} Range According to Reference 15[a]

SiC polytype	Raman band position, cm^{-1}			
	TA	LA	TO	LO
3C (β)			796	972
2H (α)	264		764, 799	968
4H (α)	196, 204, 266	610	776, 796	838, 964
6H (α)	145, 150, 236, 241, 266	504, 514	767, 789, 797	889, 965
15R (α)	167, 173, 255, 256	331, 337, 569, 577	767, 785, 797	800, 932, 938, 965

[a] Stronger bands are underlined.

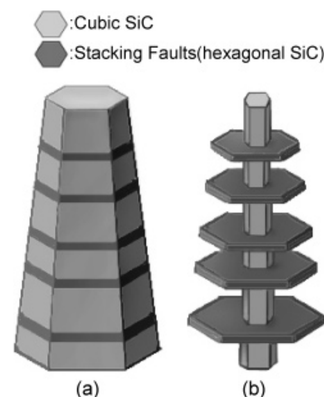

Figure 4. Schematic showing the transformation of an as-grown SiC whisker (a) to a nanostructured pagoda-like object (b) by selective etching of β-SiC.

The suggested reaction for the SiC etching process could be expressed through several steps:

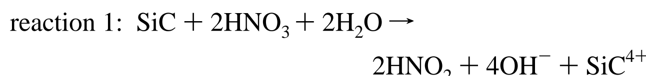

reaction 1: $SiC + 2HNO_3 + 2H_2O \rightarrow 2HNO_2 + 4OH^- + SiC^{4+}$

reaction 2: $SiC^{4+} + 4OH^- \rightarrow SiO_2 + CO_2 + 2H_2$

reaction 3: $SiO_2 + 6HF \rightarrow H_2SiF_6 + 2H_2O$

Holes produced by the oxidizing agent, HNO_3, (reaction 1) assist the oxidation (reaction 2). HF dissolves the formed oxide (reaction 3). The overall reaction with SiC is as follows:

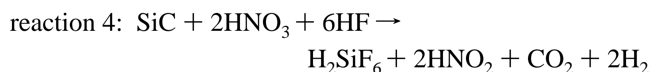

reaction 4: $SiC + 2HNO_3 + 6HF \rightarrow H_2SiF_6 + 2HNO_2 + CO_2 + 2H_2$

Differences in the sensitivity of α- and β-SiC to etching is known from several literature reports. Studies by Krasotkina et al.[18] revealed that α-SiC is stable against etching in the boiling mixture of concentrated HF, HNO_3, and H_2SO_4 acids, whereas β-SiC could be etched easily by such a mixture. Similar results were obtained by Lutsenko et al.,[19,20] who showed that β-SiC could be completely dissolved in the mixture of HF and HNO_3, whereas technical SiC powder consisting of a mixture of α- and β-SiC could be etched only partially.

Other etching methods could also express a large difference in the etching rate between α- and β-SiC (or between β-SiC and stacking faults) and thus potentially produce structures similar to those described in our paper (Figure 1). Each SiC polytype, for example, has different rates of electrochemical (e.g., anodic or photoelectrochemical) etching.[9] Electrochemical etching completely removes β-SiC but leaves porous SiC on the surface of α-SiC.[21] Different etching rates of stacking faults as compared to the bulk SiC are recognized as well. Weher et al.[22] studied defect selective etching of SiC in molten KOH/NaOH eutectic with 10% of MgO powder and electroless photoassisted etching in aqueous KOH solutions and showed that in both cases protruding etch features were formed at the intersection of stacking faults with the surface. Higher resistance of this planar defect to orthodox etching and decrease of etch rate due to recombination of charge carriers at the defects (stacking faults) in the case of photoassisted etching was suggested to explain the observed phenomena. Similar mechanisms could be responsible for the formation of SiC pagoda-like structures (Figures 1 and 4).

Electrochemical etching is well-known for expressing selectivity between SiC polytypes having different conductivities.[5,19] Electroless etching also usually exhibits p- and n-type selectivity, which was demonstrated for other wide band gap semiconductors.[23] Generally, in p-type materials the generated holes are swept away from the depleted region near the surface into the bulk of the semiconductor, thus prohibiting electroless etching.[9,19] Further studies are needed to investigate whether β-SiC parts of the whiskers (Figure 4) have doping similar to that of the stacking faults or α-SiC inclusions.

SiC nanostructures produced by this method may find numerous applications. SiC platelets produced by this method (Figure 2) are about 100−1000 times smaller than commercially produced SiC platelets.[24] Pagoda-like structures can be used in sensors. They allow a significant increase in the surface area of semiconducting SiC nanowires. They can also trap large molecules (e.g., proteins) and nanoparticles of a given size limited by spacing between the platelets. Another potential application for nanopagodas is biomedical probes, where they can be used as minimally invasive biopsy tools. The platelets will facilitate biopsy by trapping biofluids from the target tissue. The size of SiC whiskers allows probing single cells with subcellular-level resolution.

We have demonstrated the formation of separated hexagonal nanoscale SiC platelets and pagoda-like SiC nanostructures. Selective electroless etching of whiskers composed of β-SiC and periodically distributed stacking faults (α-SiC) in the mixture of HF and HNO_3 acids results in the preferential etching of β-SiC. The reproducibility of etching experiments on several kinds of commercial and experimental SiC whiskers produced in different laboratories suggests that the self-patterning phenomena are common in SiC whiskers. This process can be scaled up easily, and the proposed etching procedure can be employed in large volume production of SiC nanostructures. The produced complex SiC nanostructures have potential for use as building blocks in nanodevices. The capability of controlling the growth and etching of SiC whiskers can be applied to the fabrication of SiC-based devices including sensors and cellular probes.

Acknowledgment. We thank Dr. K. Vishnyakova for whisker samples. The purchase of the Raman spectrometer and environmental SEM was supported by NSF grants DMR-0115546 and BES-0216343, respectively. HRTEM studies were performed in Penn Regional Nanotechnology Facility, University of Pennsylvania.

References

(1) Meyer, J. A.; Baikie, I. D.; Kopatzki, E.; Behm, R. J. *Surf. Sci.* **1996**, *365*, L647.
(2) da Silva, M. J.; Quivy, A. A.; Gonzalez-Borrero, P. P.; Marega, E. *Thin Solid Films* **2002**, *410*, 188.
(3) Eymery, J.; Biasiol, G.; Kapon, E.; Ogino, T. *C. R. Phys.* **2005**, *6*, 105.
(4) Qin, L.; Park, S.; Huang, L.; Mirkin, C. A. *Science* **2005**, *309*, 113.
(5) Byun, S.; Lim, J. M.; Paik, S. J.; Lee, A.; Koo, K.; Park, S.; Park, J.; Choi, B. D.; Seo, J. M.; Kim, K.; Chung, H.; Song, S. Y.; Jeon, D.; Cho, D. *J. Micromech. Microeng*. **2005**, *15*, 1279.
(6) Shin, M. W.; Song, J. G. *Mater. Sci. Eng., B* **2002**, *95*, 191.
(7) Shor, J. S.; Osgood, R. M.; Kurtz, A. D. *Appl. Phys. Lett.* **1992**, *60*, 1001.
(8) Lauermann, I.; Memming, R.; Meissner, D. *J. Electrochem. Soc.* **1997**, *144,* 73.
(9) Haberer, E. D.; Chen, C. H.; Abare, A.; Hansen, M.; Denbaars, S.; Coldren, L.; Mishra, U.; Hu, E. L. *Appl. Phys. Lett.* **2000**, *76*, 3941.
(10) Dimitrov, R.; Tilak, V.; Yeo, W.; Green, B.; Kim, H.; Smart, J.; Chumbes, E.; Shealy, J. R.; Schaff, W.; Eastman, L. F.; Miskys, C.; Ambacher, O.; Stutzmann, M. *Solid-State Electron.* **2000**, *44*, 1361.
(11) Zhuang, D.; Edgar, J. H. *Mater. Sci. Eng., R.* **2005**, *48,* 1.
(12) Lutsenko, V. G. In *Proceedings of the NATO ARW on Synthesis, Properties and Applications of Ultrananocrystalline Diamond*; Gruen, D. M., Shenderova, O. A., Vul', A. Y., Eds.; St. Petersburg, Russia, 2005; Vol. 192, p 289.
(13) Vyshnyakova, K. L.; Pereselentseva, L. N.; Cambaz, Z. G.; Yushin, G.; Gogotsi, Y. *Br. Ceram. Trans*. **2004**, *103*, 193.
(14) Liu, Q.; Wu, K.; Geng, L.; Yao, C. K. *Mater. Sci. Eng., A* **1990**, *130*, 113.
(15) Geng, L.; Zhang, J. *Mater. Chem. Phys.* **2004**, *84,* 243.
(16) Choi, H. J.; Lee, J. G. *Ceram. Int.* **2000**, *26,* 7.
(17) Nakashima, S.; Harima, H. *Phys. Status Solidi A* **1997**, *162,* 39.
(18) Krasotkina, N. I.; Yakovleva, V. C.; Voronin, N. I.; Shmitt-Fogelevich, S. P. *Ogneupory* (in russian) **1968**, *11*, 49.
(19) Lutsenko, V. G. *Powder Metall. Met. Ceram.* **1993**, *32,*199.
(20) Beletskii, V. M.; Lutsenko, V. G.; Milkov, V. L.; Pokrovskii, D. D.; Gribkov, A. N.; Zagnitko, E. V.; Gniloshkurov, Yu. V.; Umantsev, E. L.; Gunchenko, V. M.; Polyakov, A. V. *Poroshk. Metall.* (in russian) **1986**, *5*, 44.
(21) Shor, J. S.; Kurtz, A. D.; Grimberg, I.; Weiss, B. Z.; Osgood, R. M. *J. Appl. Phys.* **1997**, *81*, 1546.
(22) Weyher, J. L.; Lazar, S.; Borysiuk, J.; Pernot, J. *Phys. Status Solidi A* **2005**, *202*, 578.
(23) Maher, H.; DiSanto, D. W.; Soerensen, G.; Bolognesi, C. R.; Tang, H.; Webb, J. B. *Appl. Phys. Lett.* **2000**, *77*, 3833.
(24) Gogotsi, Y. G.; Yoshimura, M.; Kakihana, M.; Kanno, Y.; Shibuya, M. In *Ceramic Processing Science and Technology*; Hausner, H., Messing, G. L., S. I. Hirano, Eds.; Ceramic Transactions, American Ceramic Society: Westerville, OH, 1995; Vol. 51, p 243.

NL051858V